PERGAMON

Chaos, Solitons and Fractals 11 (2000) 765–778

CHAOS
SOLITONS & FRACTALS

www.elsevier.nl/locate/chaos

Chaotic magnetic field lines in a Tokamak with resonant helical windings

R.L. Viana *

Departamento de Física, Universidade Federal do Paraná, C.P. 19081, 81531-990, Curitiba, Paraná, Brazil

Accepted 4 August 1998

Abstract

We use a Hamiltonian description for magnetic field lines in a large aspect ratio Tokamak for describing the effect of resonant helical windings in a perturbative way, taking into account the toroidal correction. We consider the formation of chains of primary (main and satellites) and secondary islands, analysing their interactions to describe the generation of chaotic magnetic field lines within a portion of the plasma column. This chaotic structure is responsible for disruptive instabilities that may spoil plasma confinement in the Tokamak. Results are compared with numerical integration of magnetic field line equations.

1. Introduction

Tokamaks are plasma confinement machines that are widely considered as promising candidates for achievement of controlled thermonuclear fusion reactions in the future. Basically they are toroidal pinches in which a plasma column is created through ohmic heating of a gas acting as the secondary of a transformer. Tokamak plasmas are confined by the simultaneous action of two basic magnetic fields: one is produced by external coils (toroidal field), and other is generated by the plasma column itself (poloidal field). Charged particles spiral along the resulting helical magnetic field lines that lie on constant pressure surfaces called magnetic surfaces, in a static magnetohydrodynamical equilibrium configuration [1].

This simple view does not take into account, however, various sources of particle and energy losses due to drifts, diffusion currents and other effects. In addition there are many kinds of instabilities, that in practice makes Tokamak confinement a challenging task for experimentalists and theoreticians [2].

One of the major problems in the obtention of long lasting plasma confinement in Tokamaks and other fusion devices is the existence of disruptive instabilities that may destroy the plasma column. The nature of these disruptive instabilities has been one of the most intriguing modern theoretical problems in Tokamak physics. One of the proposed explanations for this phenomenon is the presence of chaotic magnetic field lines in a certain portion of the plasma column, and this will be our central focus of attention [3,4].

As another example, chaotic magnetic field lines in the peripheral region of the Tokamak chamber may form a cold boundary layer that acts as an ergodic limiter, uniformizing heat and particle loading on the inner torus wall, lowering the impurity levels within the plasma core and improving confinement [5].

The understanding of how disruptive instabilities occur has augmented since the use of resonant helical windings (RHW) [6], that are conductors wound externally around the Tokamak wall with a given helicity. Disruptive instabilities in Tokamaks are typically preceded by Mirnov oscillations, which are fluctuations

* E-mail: viana@fisica.ufpr.br

0960-0779/00/$ - see front matter
PII: S0960-0779(98)00200-8

of the poloidal magnetic field that can be detected by magnetic probes [7]. The use of resonant helical windings has been proved to inhibit these oscillations below a threshold value of the perturbation [8].

It has been proposed that RHW would create a magnetic island structure within the plasma column that hinders a rotation of the MHD modes. Minor disruptions occur within the plasma in the region comprising the main island and its satellites, leading eventually to loss of confinement. The creation of a thick layer of chaotic magnetic field lines in this region is responsible for these minor disruptions [9].

The onset of chaotic behavior of magnetic field lines in a Tokamak with RHW has been studied by several authors [10–12] . The origin of chaotic field lines is the interaction between magnetic islands produced by the perturbing field on the equilibrium structure. In this work we revisit this problem from the point of view of a Hamiltonian formulation for magnetic field lines different from that used by Finn [10] in the seventies. The theory predicts that RHW would cause destruction of rational magnetic surface if toroidal effects are taken into account and the perturbation is strong enough.

The main resonance is characterized by the breaking of a resonant surface in an even number of fixed points. This structure of fixed points is the skeleton of an island chain. Each island has the characteristic structure of a nonlinear pendulum. However, when the integrability of the system is broken, as when the toroidal effect is considered, there is no longer a well-defined separatrix between librations and rotations, and a thin layer of chaotic field lines appears in this region. Diffusion is then limited by those magnetic surfaces that survives the perturbation, as explained by KAM theory. Increasing the perturbation strength turns these islands wider and eventually their stochastic layers overlap, yielding large scale chaotic motion that could trigger the disruptive instabilities that we are interested in. The terms "stochastic" and "chaotic" will be used here as synonimous, as is usually done in plasma theory and Hamiltonian dynamics.

This paper is organized as follows: in the second section we outline a Hamiltonian description for magnetic field lines due to the superposition of equilibrium and perturbing fields. Section 3 is devoted to a perturbative treatment of the magnetic island structure generated by RHW taking into account toroidal effects. In section 4 we discuss the creation of a sizeable stochastic layer near the separatrix of the main island through interaction of secondary resonances. The next section is a numerical application of the theory developed using parameters from a small Tokamak, and we describe the onset of field line stochasticity through interaction between main and satellite islands. We compare our results with numerical integration of magnetic field line equations (Poincaré surfaces of section). Our conclusions are left to the final section. An appendix describes the equilibrium and perturbing field models that have been used in this work.

2. Hamiltonian description for field-line flow

When a confined plasma has some symmetry with respect to a given coordinate, it is possible to write the magnetic field line equations, $\mathbf{B} \times \mathbf{dl} = \mathbf{0}$, in the form of Hamilton's equations of motion. We are considering static equilibrium situations, so the role of time is played by the ignorable, or cyclic, coordinate. The remaining spatial and/or magnetic flux coordinates give the canonical position and momentum variables. The advantage of this procedure is that one can use the powerful methods of Hamiltonian dynamics, like perturbation theory, KAM theory, adiabatic invariance, etc. to analyse magnetic field topology when a static magnetic perturbation is applied on a given equilibrium field.

This analogy was first pointed out by Kerst [13], and later used to describe the effect of non-symmetric perturbations in various plasma confinement machines: Stellarators [14], Levitrons [15] and Tokamaks [10,16]. A Hamiltonian description valid in an arbitrary curvilinear coordinate system is also available [17], and it has been applied for magnetic fields with helical symmetry [18] and spherical symmetry [19], the latter being relevant for some compact tori models (Spheromaks and FRC). We have also used this formalism to describe the action of an ergodic magnetic limiter in the peripheral region of a Tokamak [20].

The magnetic field lines are parametrized by the timelike variable, in the sense that what could be called "field line flow" is, in fact, a Lagrangean description of a magnetostatic situation. Regular dynamics is characterized by the presence of a nested set of magnetic surfaces which correspond to KAM tori. A generic static perturbation will spoil the integrability of field line motion, through the destruction of rational tori

(according to Poincaré–Birkhoff theorem) and the creation of chains of islands associated with resonances between the perturbing modes and the equilibrium field line motion [21].

In this framework it is possible to characterize chaotic motion since two field lines originally very close may separate exponentially after a large number of revolutions along the torus, and the field lines wander by a region of the available phase space. The perturbed field line flow is a nonautonomous one degree of freedom Hamiltonian system, so chaotic motion can appear in the vicinity of island separatrices or over an extended portion of the phase space if adjacent islands interact.

Tokamaks with a large aspect ratio can be described, in a first approximation, by a periodic cylinder model. It is possible to consider the toroidal correction as a perturbing effect, acting on an equilibrium model described by cylindrical geometry. The toroidal correction is expanded in a sum of terms proportional to powers of the inverse local aspect ratio, and it multiplies the perturbing Hamiltonian calculated through a lowest order approximation. This method has led to a successful analysis of the role of the magnetic stochasticity in the so-called sawtooth oscillations [22,23].

Let us consider the "local", or "pseudo-toroidal" coordinates (r, θ, ϕ), as depicted in Fig. 1. R_0 and b denote the Tokamak major and minor radii, and $a < b$ is the plasma column radius set by a material limiter. The plasma aspect ratio R_0/a is supposed to be large enough to justify our approximations. The magnetic field line equations are written in these local coordinates as

$$\frac{\mathrm{d}r}{B_r} = \frac{r\mathrm{d}\theta}{B_\theta} = \frac{R\mathrm{d}\phi}{B_\phi}, \tag{1}$$

where $R = R_0 + r\cos\theta$.

The cylindrical approximation will be taken as our "exactly solved" case for the perturbative treatment. Axisymmetry implies that the toroidal angle ($0 \leqslant \phi < 2\pi$) is an adequate time variable, whereas the poloidal angle ($0 \leqslant \theta < 2\pi$) is the position variable. The momentum canonically conjugated to θ is a function of the magnetic surface radius: $J = r^2/2$, since the magnetic surfaces have circular and concentric cross-sections.

The equilibrium magnetic field in lowest order is $\mathbf{B}^{(0)} = (0, B_\theta^{(0)}(r), B_0)$, in which $B_0 = B_\phi^{(0)}$ is the (uniform) toroidal field produced by external coils, and $B_\theta^{(0)}(r)$ is the poloidal field created by the plasma column. The magnetic field line equations Eq. (1) related to this equilibrium model are written as a pair of canonical equations

$$\frac{\mathrm{d}J}{\mathrm{d}\phi} = -\frac{\partial H_0}{\partial\theta}, \tag{2}$$

$$\frac{\mathrm{d}\theta}{\mathrm{d}\phi} = \frac{\partial H_0}{\partial J}, \tag{3}$$

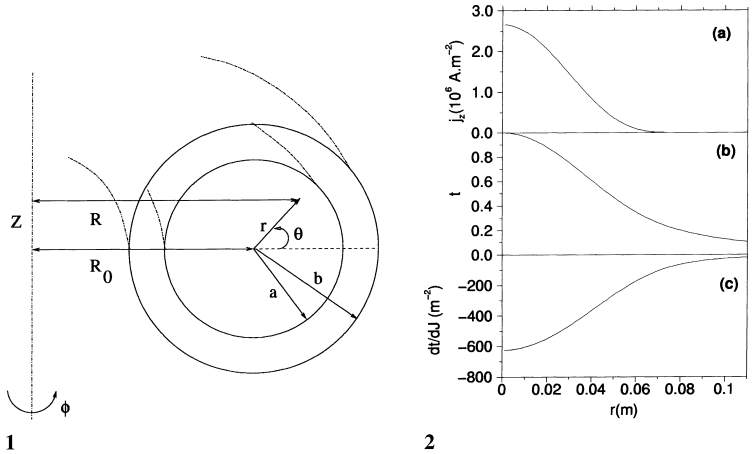

Fig. 1. Local coordinates for a Tokamak.

Fig. 2. Radial profiles for: (a) plasma current density; (b) rotational transform; (c) magnetic shear, using TBR-1 parameters.

referring to an unperturbed Hamiltonian

$$H_0(J) = \int_0^J t(J')\,\mathrm{d}J', \tag{4}$$

which is written in terms of the (normalized) rotational transform

$$t(J) = \frac{1}{q(J)} = \frac{1}{2\pi}\int_0^{2\pi}\frac{\mathrm{d}\theta}{\mathrm{d}\phi}\mathrm{d}\phi = \frac{R_0 B_\theta^{(0)}(J)}{\sqrt{2J}B_0}. \tag{5}$$

and $q(r)$ is the so-called safety factor of the magnetic surfaces. As the unperturbed Hamiltonian Eq. (4) is cyclic in θ, the corresponding momentum is a constant of motion, and (J,θ) are actually action-angle variables.

The perturbation Hamiltonian refers to the field produced by a RHW. The field components are written as $\mathbf{B}^{(1)}(r,\theta,\phi) = h_s^{-1}(b_r^{(1)}, b_\theta^{(1)}, b_\phi^{(1)})$, with the components of $\mathbf{b}^{(1)}$ being calculated in the cylindrical approximation, and

$$\frac{1}{h_s(r,\theta)} = \left(1 + \frac{r}{R_0}\cos\theta\right)^{-1} = \sum_k \left(-\frac{r}{R_0}\right)^{|k|} \mathrm{e}^{\mathrm{i}k\theta} \tag{6}$$

is the toroidal correction [14].

The field line behavior is then governed by a near-integrable Hamiltonian

$$H(J,\theta,\phi) = H_0(J) + H_1(J,\theta,\phi), \tag{7}$$

in which the perturbation Hamiltonian H_1 is written in the action-angle variables of the unperturbed system, and $|H_1| \ll |H_0|$. We apply the toroidal correction to this term, writing it as h_1/h_s, where

$$h_1(J,\theta,\phi) = \sum_{m',n'} A_{m'n'}(J)\mathrm{e}^{\mathrm{i}(m'\theta - n'\phi)} \tag{8}$$

is the Fourier expansion of the perturbation, supposed periodical in both angles.

Combining Eq. (6), Eq. (8), the perturbing Hamiltonian in local coordinates is

$$H_1(J,\theta,\phi) = \sum_{k,m',n'} \left(-\frac{\sqrt{2J}}{R_0}\right)^{|k|} A_{m'n'k}(J)\mathrm{e}^{\mathrm{i}(m'+k)\theta}\mathrm{e}^{-\mathrm{i}n'\phi}, \tag{9}$$

whose Fourier coefficients are related to the coefficients of the radial perturbing field component $b_{\mathrm{r}m'n'}(J)$ by

$$A_{m'n'k}(J) = -\frac{\sqrt{2J}R_0 b_{\mathrm{r}m'n'}(J)}{i(m'+k)B_0}, \tag{10}$$

since, from Eq. (2), we have

$$\frac{\partial H_1(J,\theta,\phi)}{\partial\theta} = -\sqrt{2J}\frac{R_0 B_r^{(1)}(J,\theta,\phi)}{B_0}. \tag{11}$$

3. Main and satellite primary islands

The main effect of a RHW with m pairs of equally spaced windings, that close on themselves after n turns along the poloidal direction, is to excite one harmonic with mode numbers $(m',n') = (m,n)$. Hence the summation in H_1 will run only over the toroidal correction. We shall pick up the lowest order term $k = 0$ (straight helical field) to put into evidence the main resonance caused by such a RHW

$$H(J,\theta,\phi) = H_0(J) + A_{mn0}(J)\mathrm{e}^{\mathrm{i}(m\theta - n\phi)} + \sum_{k\neq 0}\left(-\frac{\sqrt{2J}}{R_0}\right)^{|k|} A_{mnk}(J)\mathrm{e}^{\mathrm{i}(m+k)\theta}\mathrm{e}^{-\mathrm{i}n\phi}. \tag{12}$$

Let us expand this Hamiltonian around an unperturbed orbit characterized by $(J,\theta)=(J_0,t_0\phi)$, where t_0 is the rotational transform calculated for $J=J_0$,

$$J=J_0+\Delta J,\qquad \theta=t_0\phi+\Delta\theta. \tag{13}$$

Linearizing the canonical equations Eq. (2) we have

$$\frac{\mathrm{d}\Delta J}{\mathrm{d}\phi}\approx-\frac{\partial H_1(J_0,\theta,\phi)}{\partial\theta},\quad \frac{\mathrm{d}\Delta\theta}{\mathrm{d}\phi}\approx\left.\frac{\mathrm{d}t}{\mathrm{d}J}\right|_{J_0}\Delta J. \tag{14}$$

The helical perturbation caused by a (m,n) RHW will break the unperturbed magnetic surface located at $J=J_0$ with a resonance between poloidal and toroidal field line motion

$$m\theta-n\phi=2\pi\kappa,\quad(\kappa\in Z), \tag{15}$$

that implies a rational value for the local rotational transform, i.e, $t_0=n/m$.

Let ΔH be the Hamiltonian of field line motion around this resonant surface. From Eq. (14) it is written as

$$\Delta H(\Delta J,\theta,\phi)=t_0\Delta J+\left.\frac{\mathrm{d}t}{\mathrm{d}J}\right|_{J_0}\frac{(\Delta J)^2}{2}+A_{mn0}(J_0)\mathrm{e}^{\mathrm{i}(m\theta-n\phi)}+\sum_{k\neq0}\left(-\frac{\sqrt{2J_0}}{R_0}\right)^{|k|}A_{mnk}(J_0)\mathrm{e}^{\mathrm{i}(m+k)\theta}\mathrm{e}^{-\mathrm{i}n\phi}. \tag{16}$$

The primary resonance Eq. (15) may be removed by going to a rotating frame through a canonical transformation to new variables $(\Delta\hat{J},\hat{\theta},\phi)$ with a generating function $F_2(\Delta\hat{J},\theta,\phi)=(m\theta-n\phi)\Delta\hat{J}$. The transformation equations are [24]

$$\hat{\theta}=m\theta-n\phi,\quad \Delta J=m\Delta\hat{J}, \tag{17}$$

$$\Delta\hat{H}(\Delta\hat{J},\hat{\theta},\phi)=\Delta H(\Delta J,\theta,\phi)-mt_0\Delta\hat{J}. \tag{18}$$

Substituting these hatted variables in Eq. (16) and averaging $\Delta\hat{H}(\Delta\hat{J},\hat{\theta},\phi)$ over the fast variable ϕ, we find the Hamiltonian that describes the averaged motion around the main resonance (m,n)

$$K_0(\Delta\hat{J},\hat{\theta})=\langle\Delta\hat{H}(\Delta\hat{J},\hat{\theta},\phi)\rangle_\phi=\frac{G}{2}(\Delta\hat{J})^2-F\cos\hat{\theta}, \tag{19}$$

where we have defined

$$F\equiv-A_{mn0}(J_0),\quad G\equiv m^2\left.\frac{\mathrm{d}t}{\mathrm{d}J}\right|_{J_0}. \tag{20}$$

Eq. (19) is the pendulum Hamiltonian, characterizing the main island (m,n). Looking at the separatrix connecting the hyperbolic fixed points at $\hat{\theta}=\pm\pi$ we obtain the amplitude, or half-width, of this resonance

$$\Delta\hat{J}_M=2\left|\frac{F}{G}\right|^{1/2}, \tag{21}$$

as well as the frequency at the elliptic singular point $\hat{J}=0$ (or $J=J_0$):

$$\omega_0=|FG|^{1/2}. \tag{22}$$

Supposing that $r_0/R_0\ll1$, when considering the effects of the toroidal correction it would suffice to look at small k values in Eq. (12), i.e. $k=\pm1$. They produce terms with angular dependences $\mathrm{e}^{\mathrm{i}(m\pm1)\theta-\mathrm{i}n\phi}$. The same reasoning applied for the main resonance leads that these perturbation modes $(m\pm1,n)$ induced by the toroidal correction generate satellite islands, centred at resonant unperturbed surfaces with rotational transforms given by $n/(m\pm1)$.

We now proceed in a similar way as we have done for the main island, picking up either one of the two possible satellite modes in Eq. (12) and linearizing around the new resonance positions in action space. Then we transform to a rotating frame through new canonical transformations: $\hat{\theta}=(m\pm1)\theta-n\phi$,

$\Delta J = (m \pm 1)\Delta\hat{J}$, average over ϕ and reobtain the pendulum Hamiltonian for the satellite islands, with half-widths and frequencies given, respectively, by

$$\Delta\hat{J}_{\mathrm{MP}} = 2\left|\frac{F_{\mathrm{P}}}{G_{\mathrm{P}}}\right|^{1/2}, \quad \omega_{0\mathrm{P}} = |F_{\mathrm{P}}G_{\mathrm{P}}|^{1/2}, \tag{23}$$

with

$$F_{\mathrm{P}} \equiv \frac{\sqrt{2J_0}}{R_0}A_{mn,\pm1}(J_0), \quad G_{\mathrm{P}} \equiv (m \pm 1)^2\left.\frac{\mathrm{d}t}{\mathrm{d}J}\right|_{J_0}. \tag{24}$$

Let us suppose (see Appendix A) that the safety factor is a monotonically increasing function of r. Calling $r_0^{(k)}$ the location of the resonant surface ($k = 0$ means no toroidal effect), we have the ordering $r_0^{(-1)} < r_0^{(0)} < r_0^{(+1)}$, which also holds for the action variable.

4. Second order resonances and the stochastic transition

Once we have determined the structure of the primary resonances caused by the action of a RHW, we can proceed further and investigate the structure of the secondary resonances between the primary island oscillation frequency and the fast fundamental frequency of field line motion. Considering those terms in the Hamiltonian describing the motion around the main resonance in the hatted variables of the island rotating frame, but that were not averaged out in ϕ, we have

$$\begin{aligned} K(\Delta\hat{J},\hat{\theta},\phi) &= K_0(\Delta\hat{J},\hat{\theta}) + K_1(\Delta\hat{J},\hat{\theta},\phi) \\ &= K_0(\Delta\hat{J},\hat{\theta}) + \sum_{k\neq0}\left(-\frac{\sqrt{2J_0}}{R_0}\right)^{|k|}A_{mnk}(J_0)\mathrm{e}^{i\left[\left(\frac{k}{m}+1\right)\hat{\theta}+\frac{kn}{m}\phi\right]}, \end{aligned} \tag{25}$$

and K_0 is the pendulum Hamiltonian Eq. (19) that was used to compute the amplitude and frequency of the main island. Now we transform to action-angle variables in the pendulum frame (I,ϑ) by means of the canonical transformation

$$\hat{\theta} = \left(\frac{2I}{\bar{R}}\right)^{1/2}\sin\vartheta, \tag{26}$$

$$\hat{J} = \left(2\bar{R}I\right)^{1/2}\cos\vartheta, \tag{27}$$

in which $\bar{R} \equiv |F/G|^{1/2}$. Using these new variables it is possible to express the pendulum Hamiltonian Eq. (19) in terms of the action I only. We can use an approximate expression obtained through first-order canonical perturbation theory [21]

$$K_0(I) = \omega_0 I - \frac{1}{16}GI^2, \tag{28}$$

where ω_0 is the frequency of the exact resonance at J_0. The nonaveraged terms are, in these new action-angle variables,

$$\begin{aligned} K_1(I,\vartheta,\phi) &= \sum_{k\neq0}a_k\exp\left\{i\left[\left(\frac{k}{m}+1\right)\left(\frac{2I}{\bar{R}}\right)^{1/2}\sin\vartheta+\frac{kn}{m}\phi\right]\right\} \\ &= \sum_{k\neq0}a_k\sum_{\ell}\mathscr{J}_{\ell}\left[\left(\frac{k}{m}+1\right)\left(\frac{2I}{\bar{R}}\right)^{1/2}\right]\mathrm{e}^{i\left(\ell\vartheta+\frac{kn}{m}\phi\right)}, \end{aligned} \tag{29}$$

with coefficients

$$a_k \equiv \left(-\frac{\sqrt{2J_0}}{R_0}\right)^{|k|}A_{mnk}(J_0), \tag{30}$$

and $\mathscr{J}_m(\chi)$ is the Bessel function of order m.

Since $r_0/R_0 \ll 1$ we need only small values of k, so we retain the $k = \pm 1$ terms in Eq. (29). A secondary resonance, centred at $I = I_0$, is characterized by a relation between the primary island oscillation frequency

$$\omega(I) = \frac{\mathrm{d}\vartheta}{\mathrm{d}\phi} = \frac{\mathrm{d}K_0}{\mathrm{d}I} = \omega_0 - \frac{G}{8}, \tag{31}$$

and the "fast" fundamental frequency $\omega_\phi = 1$, in the following form

$$\ell\omega(I_0) - \frac{n}{m} = 0. \tag{32}$$

Picking only this ℓ-resonance out of the Hamiltonian K, and considering $a_{-1} \approx a_1$, we have

$$K(I,\vartheta,\phi) = K_0(I) + a_1 V_{\ell 1}(I)\cos\left(\ell\vartheta - \frac{n}{m}\phi\right) + \sum_{\alpha\neq\ell} a_1 V_{\alpha 1}(I)\mathrm{e}^{\mathrm{i}(\alpha\vartheta - \frac{n}{m}\phi)}, \tag{33}$$

in which the Bessel coefficients are

$$V_{\ell k}(I) \equiv \mathscr{J}_\ell\left[\left(\frac{k}{m}+1\right)\left(\frac{2I}{\bar{R}}\right)^{1/2}\right]. \tag{34}$$

such that $V_{\ell,-1} \approx V_{\ell 1}$.

Expanding around the secondary resonance, $I = I + \Delta I$, going to the rotating frame variables through the canonical transformation

$$\hat{\vartheta} = \ell\vartheta - \frac{n}{m}\phi, \qquad \hat{I} = \frac{I}{\ell}, \tag{35}$$

and averaging over ϕ, there results the pendulum Hamiltonian characterizing the secondary island ($\Delta K = K - K_0(I_0)$)

$$\mathscr{H}_0(\Delta\hat{I},\hat{\vartheta}) = \langle\Delta\hat{K}(\Delta\hat{I},\hat{\vartheta},\phi)\rangle_\phi = \frac{G_\mathrm{s}}{2}(\Delta\hat{I})^2 - F_\mathrm{s}\cos\hat{\vartheta}, \tag{36}$$

in which

$$F_\mathrm{s} \equiv -a_1 V_{\ell 1}(I_0), \quad G_\mathrm{s} \equiv \ell^2\left.\frac{\mathrm{d}^2 K_0}{\mathrm{d}I^2}\right|_{I_0} = -\ell^2\frac{G}{8}. \tag{37}$$

The half-width and frequency of this secondary resonance are thus

$$\Delta\hat{I}_M = 2\left|\frac{F_\mathrm{s}}{G_\mathrm{s}}\right|^{1/2}, \quad \hat{\omega}_0 = |F_\mathrm{s}G_\mathrm{s}|^{1/2}. \tag{38}$$

We may interpret the stochastic layer around the separatrix of the main (m,n) island as the result of the interaction of two neighboring secondary resonances near the separatrix, with mode numbers ℓ and $\ell+1$. Previous studies, including field-line Hamiltonians [22], have shown that if $\ell > 6$ a sizeable stochastic layer is formed in the peripheral region of the main (m,n) island.

For weak perturbation, field line excursions along this stochastic layer are limited by the fact that there are undestructed magnetic surfaces between the main and satellite islands. They act as "dikes", preventing large scale field line motion. Global stochasticity, on the other hand, is characterized by interconection of the stochastic layers of the main island and any of its satellites. There are many criteria for determining the onset of global stochasticity through island overlapping [25], renormalization of the phase space between islands [26] or residue analysis [27].

One can study the interaction of the primary islands in parallel with the interaction of the secondary islands of the main resonance, thanks to a universal relation characteristic of the pendulum approximation.

Let us define a stochasticity parameter relating the ratio of the sum of the ℓ and $\ell+1$ secondary island amplitudes to their mutual distance

$$S_s = \frac{\Delta\hat{I}_{M,\ell} + \Delta\hat{I}_{M,\ell+1}}{|\hat{I}_{0,\ell} - \hat{I}_{0,\ell+1}|} \approx \frac{2\Delta I_M}{\delta I}, \tag{39}$$

in which we have taken off the hats on the variables since we are computing their ratio. It is also supposed here that $\Delta I_{M,\ell} \approx \Delta I_{M,\ell+1} \equiv \Delta I_M$, and we define $\delta I = |I_{0,\ell} - I_{0,\ell+1}|$.

It is possible to prove a relation between the frequencies of the primary and secondary island oscillations [21]

$$S_s = \frac{4\hat{\omega}_0}{\omega_0} = 4\alpha_0 = \frac{4}{Q_0}, \tag{40}$$

in which α_0 is the local rotation number, being the inverse of the number of orbits per libration period Q_0. This relation is universal in the sense that it is valid for all neighboring island chains of any order. In particular, it shall apply to the primary islands, that generates the global stochasticity scenario we are studying.

In the next section we will integrate numerically the field line equations to investigate the merging of large scale stochasticity and find that this transition occurs near the appearance of a set of five secondary islands (see Fig. 8 for an example). Thus $Q_0 = 5$, implying that the threshold value of the stochasticity parameter (that is the same for both primary and secondary chains) is $(S_s)_{crit} = 4/5 = 0.8$.

On the other hand, there are claims that this critical value would be $2/3$ (the so-called "two-thirds" rule), that corresponds to a set of six second-order islands near stochasticity (i.e., $Q_0 = 6$) [21]. Our results, however, are not in contradiction with this claim, since it has been made for cases in which the interacting islands have similar widths, as in the standard map [25]. For interactions between a main resonance and one of its satellites, the toroidal effect implies a significant difference between their widths, so the $2/3$-rule is no longer accurate in these cases.

5. Numerical results

In the following numerical application we will take some parameters from the small Tokamak TBR-1, operating at Universidade de São Paulo, Brazil [28] (see Table 1). TBR-1 discharges in the plateau regime can be modelled, in lowest order, by a peaked current density profile

$$j_z(r) = \begin{cases} j_0\left(1 - \frac{r^2}{a^2}\right)^\gamma, & (0 \leqslant r \leqslant a) \\ 0, & (a \leqslant r \leqslant b) \end{cases} \tag{41}$$

in which j_0 and γ are positive parameters.

Table 1
Main parameters of the TBR-1 Tokamak

Parameter	Value
Major radius (R_0)	0.30 m
Minor radius (b)	0.11 m
Plasma radius (a)	0.08 m
Toroidal field (B_0)	0.5 T (at magnetic axis)
Safety factor (q_a)	5.0 (at plasma edge)
Plasma current (I_P)	10.0 kA (typical value)
Pulse duration (τ_P)	7–9 ms
Central electron temperature (T_{e0})	200 eV
Central electron density (n_{e0})	$7.0 \times 10^{18}\mathrm{m}^{-3}$
Filling pressure (p)	10^{-4} torr

The θ-averaged safety factor $q(r) = 1/t(r)$ produced by such a profile is obtained in Appendix A. At the plasma edge its value is given by $q_a = q(a) = q(0)(\gamma + 1)$. The Kruskal–Shafranov criterion for absence of internal kink modes [2] states that, at the magnetic axis, $q(0) \geqslant 1$, so we choose $q(0) = 1$ in order to satisfy this requirement. With this constraint the remaining equilibrium properties are determined by γ, which gives the shape of the current profile. For typical TBR-1 discharges it has been estimated that $q_a \approx 5.0$ [28]. Fig. 2 shows the radial profiles for current density, rotational transform, and its derivative (magnetic shear), using TBR-1 parameters.

The external magnetostatic perturbation to be studied here is due to a RHW with $m = 3, n = 1$ (Fig. 3). There will be a chain of three primary islands centred at the surface for which the rotational transform is $1/3$. We have seen in the previous section that there will appear, due to the toroidal correction, at least two sizeable satellite island chains, centred at those surfaces with $t_0 = 1/2$ and $1/4$. Fixing $q(0) = 1$, we can compute the radial locations of these surfaces with respect to variations in γ, that is the tunable parameter of the equilibrium model field (Fig. 4).

As $t(r)$ is a monotonically decreasing function of the radius (see Fig. 2), the relative positions of the main and satellite islands are only slightly unchanged even for large variation of γ. For $\gamma = 4$, the main and satellite islands are located in the annulus $0.56 \lessapprox (r_0/a) \lessapprox 0.94$, occupying roughly the outer half of the plasma column. This is convenient to model effects related to disruptive instabilities, as has been done in previous works [11], like interactions between islands with a material limiter or other islands.

The magnetic field generated by a (m, n) RHW is shown in Appendix A. We suppose that this field is superposed to the equilibrium field in a simple way, $\mathbf{B} = \mathbf{B}^{(0)} + \mathbf{B}^{(1)}$, neglecting plasma response. For marginally stable states, when this response is not negligible, this approximation may not be admissible. Considering the toroidal effect on the radial perturbation field component, we have for the Fourier coefficient of the Hamiltonian expansion in Eq. (12)

$$A_{mnk}(J) = -\frac{\epsilon}{m+k}\left(\frac{\sqrt{2J}}{b}\right)^m, \tag{42}$$

in which we have used Eq. (10), (A.13), and defined

$$\epsilon = \frac{\mu_0 I_H R_0}{\pi B_0} \tag{43}$$

as a measure of the perturbation strength. The half-widths (in action space) of the main and satellite island generated by a $(3, 1)$ RHW are given by Eqs. (21) and (22) and are depicted in Fig. 5 for different values of the winding current I_H. These amplitudes in the physical space are computed through

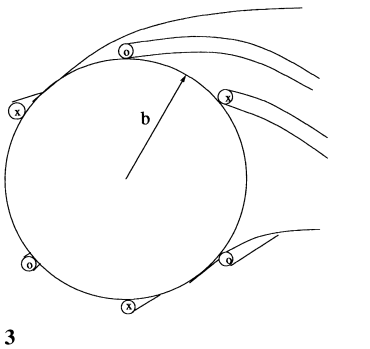

3

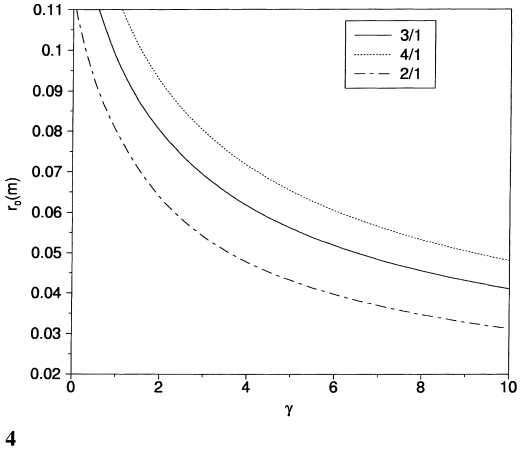

4

Fig. 3. Resonant helical windings with $m = 3$.

Fig. 4. Radial location of some rational unperturbed magnetic surfaces as a function of current profile exponent for TBR-1 parameters ($\gamma = q_a - 1$).

$$\Delta r_{\mathrm{M}} = \sqrt{2}\left(\sqrt{\Delta J_M + J_0^{(0)}} - \sqrt{J_0^{(0)}}\right), \tag{44}$$

$$\Delta r_{\mathrm{MP}}^{(\pm 1)} = \sqrt{2}\left(\sqrt{\Delta J_{\mathrm{MP}}^{(\pm 1)} + J_0^{(\pm 1)}} - \sqrt{J_0^{(\pm 1)}}\right). \tag{45}$$

in which $J_0^{(k)}$ is the location of the corresponding resonant surface.

For main and satellite islands the amplitude increases with $I_H^{1/2}$, but the toroidal correction introduces a factor proportional to $(r_0/R_0)^{m/2}$ which decreases substantially the satellite half-widths when compared with the main island. The onset of magnetic field line stochasticity between the main and either of its satellites is describing by analysing the corresponding stochasticity parameter

$$S_{\mathrm{p}} = \frac{\Delta J_{\mathrm{M}} + \Delta J_{\mathrm{MP}}^{(\pm 1)}}{|J_0^{(0)} - J_0^{(\pm 1)}|}. \tag{46}$$

Numerical observations of the islands behavior near the transition has pointed that $(S_{\mathrm{p}})_{\mathrm{crit}} = (S_{\mathrm{s}})_{\mathrm{crit}} \approx 0.8$. Fig. 5(b) shows the stochasticity parameters for overlapping of the 3/1 main resonance with its two satellites, as a function of the helical current. It indicates a critical current of about $140A$ for the (3,1)–(4,1) pair and $260A$ for the (4,1) satellite. As these currents are actually slightly higher, an improved critical value of about 0.85 would better describe the onset of global stochasticity.

In order to verify our theoretical results obtained through application of Hamiltonian perturbation theory, we have integrated numerically the magnetic field line equations Eq. (1) using the equilibrium and helical winding fields shown in the Appendix A. We present the results of a Poincaré surface of section map $(r \times \theta)$ of field lines at $\phi = 0$. Fig. 6 shows the phase portrait for a helical current of $90A$. The main island 3/1 shows up, as well as their satellites, with locations and amplitudes in good agreement with the theoretical values.

Notice that the main island has a quite sizeable stochastic layer, but there are some remaining magnetic surfaces isolating it from their satellites. In this case, we can see that a thick stochastic layer is formed in the $(3,1)$ main island, through interaction of $\ell = 6$ and 7 second-order resonances, since the $\ell = 5$ chain is still visible.

For higher currents, as in Fig. 7, both $(3,1)$ and $(4,1)$ have sizeable stochastic layers, but they are not connected, as required for global stochasticity. There is at least one KAM tori isolating these stochastic

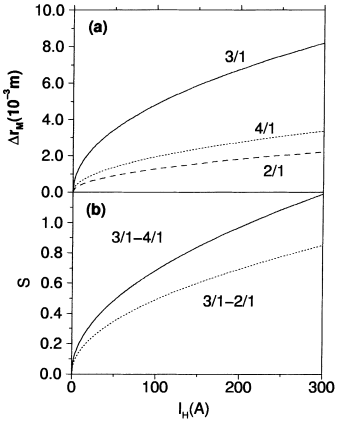

5

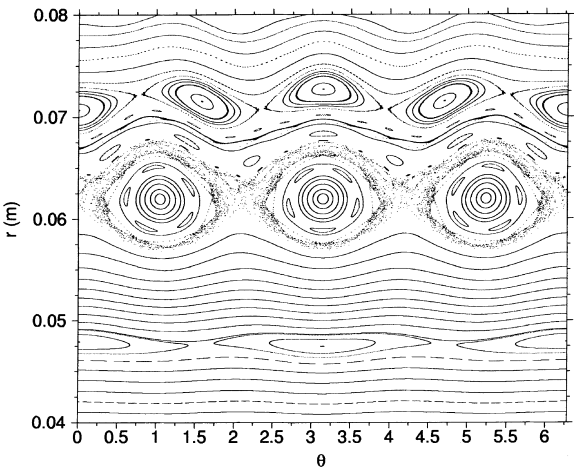

6

Fig. 5. (a) Half-widths of main and satellite islands for TBR-1 parameters and $\gamma = 4.0$ as a function of the helical winding current; (b) stochasticity parameters for interactions of main and satellite islands.

Fig. 6. Poincaré surface of section for magnetic field lines $(\phi = 0)$ in a Tokamak with a $(3,1)$ resonant helical limiter. TBR-1 parameters are used, with $\gamma = 4.0$ and an helical current of $I_{\mathrm{H}} = 90A$.

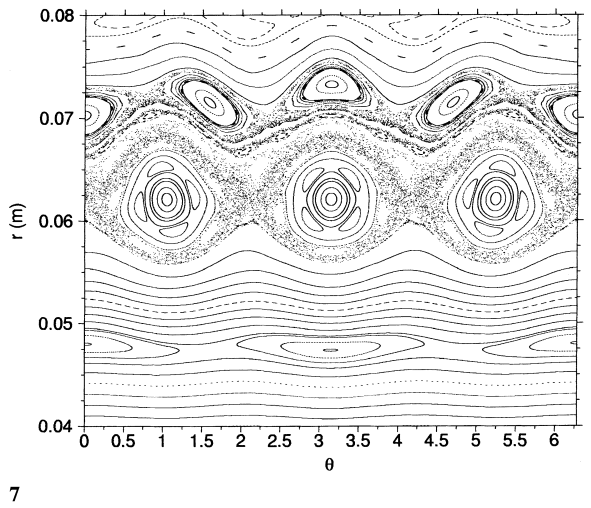

7

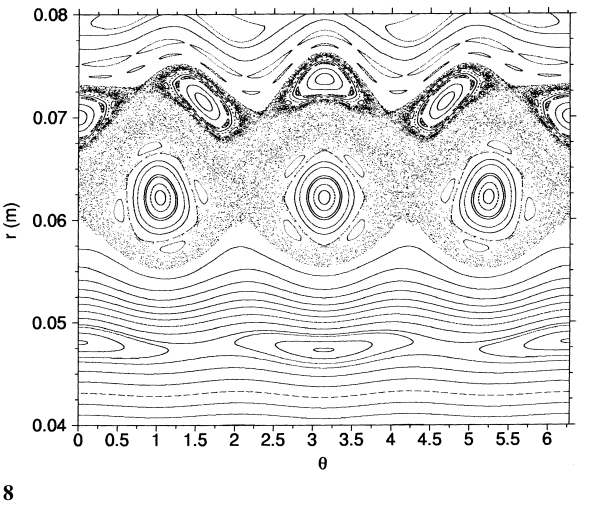

8

Fig. 7. Poincaré map of field lines for $I_{\mathrm{H}} = 130A$ and $\gamma = 4.0$.
Fig. 8. Poincaré map of field lines for $I_{\mathrm{H}} = 160A$ and $\gamma = 4.0$.

layers. Only for $I_H \approx 160A$ (Fig. 8) we can see the onset of global stochasticity since the two island layers interconnect, i.e., field lines wander ergodically through a region comprising both resonances. Near these values the set of five secondary resonances has already overlapped, so we have taken a local rotation number of $\alpha_0 = 1/5$ in the criterion (Eq. (40)) for the stochastic transition.

From Fig. 5, we also see that the helical current needed to obtain global stochasticity between $(3,1)$ and $(2,1)$ islands is very large compared with the other satellite, so there is little interest in considering this possibility as the main cause of stochasticity due to this RHW.

6. Conclusions

The effect of a RHW on the magnetic field line structure in a Tokamak is the generation of chains of islands, centred at resonant magnetic surfaces. The interaction of these islands may produce a region where there are chaotic magnetic field lines, if the perturbation is large enough. Field line chaos is related to disruptive instabilities triggered by such windings, and it has been used as an experimental tool to study this phenomenon. Due to the Hamiltonian character of field line motion, we have considered this problem from the point of view of canonical perturbation theory, as has been done in theoretical studies of sawtooth oscillations [22,23]. Previous works on the same subject [10] have considered different Hamiltonian formulations, model fields, and alternative methods to compute island structure [11,12].

We assume, as Lichtenberg [22], the large aspect ratio limit as the unperturbed, soluble Hamiltonian problem, in which the magnetic surfaces have circular and concentric cross-sections. A peaked model for the plasma current density is considered, depending on two variable parameters: the safety factor at the magnetic axis $q(0)$, and a shape parameter γ, related to the value of $q(r)$ at the plasma edge. Toroidal corrections are inserted in the perturbing Hamiltonian, besides the helical winding field. The latter is obtained by considering pairs of conductors wound around the Tokamak, conducting currents of opposite senses for adjacent windings.

The main resonance produced by this RHW is characterized by mode numbers $(3,1)$. Satellite islands $(4,1)$ and $(2,1)$ are created due to the toroidal correction. We interpret the generation of global stochasticity in the region around the main resonance as the interaction of $(3,1)$ and $(4,1)$ islands.

Numerical integration of field line equations indicates that the onset of global stochasticity between these primary resonances occurs for a helical current of about $160A$, which is less than 2% of the total plasma current, being a reasonable value for practical operation of such a device. We have also analysed the secondary resonances between the primary island oscillation frequency and the "fast" frequency. A sizeable

stochastic layer is present when one considers mode numbers for second order islands higher than six, which is a standard result in Hamiltonian theory, and is confirmed by numerically obtained Poincaré surfaces of section.

The transition between local and global stochasticity occurs for a local rotation number near $1/5$, so the critical stochasticity parameter was estimated to be nearly equal to 0.85, which is higher than the $2/3$ limit that is strictly valid only for islands of equal amplitude, which is not our case due to the differences created by toroidal correction.

Our criterion for determining this transition has been essentially heuristic, since it relies on numerical results. More accurate estimates for the critical perturbation strength would need the use of a more sophisticated criterion, like that furnished by the Escande–Doveil renormalization method [26,29] or by residue analysis [27]. The method developed here could also work with different geometries, as the toroidal coordinate system [30], as well as other models for equilibrium fields.

Acknowledgements

This work was made possible by partial finantial support of CNPq (Conselho Nacional de Desenvolvimento Científico e Tecnológico) – Brazil and the National Science Foundation – United States, through a joint research project. The author would like to acknowledge Dr. S.R. Lopes for valuable discussions.

Appendix A. Equilibrium and perturbing model fields

Using the cylindrical approximation to compute equilibrium field parameters, we consider the plasma current density profile $\mathbf{j} = j_z(r)\hat{e}_z$, where j_z is given by the peaked model, Eq. (41). The poloidal field created by such current is

$$B_\theta^{(0)}(r) = \begin{cases} \frac{\mu_0 j_0 a^2}{2(\gamma+1)r}\left[1 - \left(1 - \frac{r^2}{a^2}\right)^{\gamma+1}\right], & (0 \leqslant r \leqslant a) \\ \frac{\mu_0 I_P}{2\pi r}, & (a \leqslant r \leqslant b) \end{cases} \tag{A.1}$$

in which $I_P = \pi a^2 j_0/(\gamma+1)$ is the total plasma current.

In this lowest order treatment of the equilibrium field, the cross-sections of the unperturbed magnetic surfaces are concentric circles. The normalized rotational transform of these surfaces is given by Eq. (5), which gives for this model

$$t(r) = \begin{cases} \frac{1}{q_a}\frac{a^2}{r^2}\left[1 - \left(1 - \frac{r^2}{a^2}\right)^{\gamma+1}\right], & (0 \leqslant r \leqslant a) \\ \frac{1}{q_a}\frac{a^2}{r^2}, & (a \leqslant r \leqslant b) \end{cases} \tag{A.2}$$

in which $q_a = (2\pi B_0 a^2)/(R_0 \mu_0 I_P)$ is the safety factor at plasma edge.

The radial location of the resonant surfaces with mode numbers (m,n) is given by

$$q_a \frac{r_0^2}{a^2}\left\{1 - \left[1 - \frac{r_0^2}{a^2}\right]^{\gamma+1}\right\}^{-1} = \frac{m}{n}, \quad \left(1 \leqslant \frac{m}{n} \leqslant q_a\right), \tag{A.3}$$

$$r_0 = a\sqrt{\frac{m}{q_a n}}, \quad \left(q_a \leqslant \frac{m}{n} \leqslant q_b\right), \tag{A.4}$$

where $q_b = (b/a)^2 q_a$ is the safety factor at the Tokamak inner wall.

Using Eq. (4), it is not possible to obtain a closed form for the unperturbed Hamiltonian in this model for arbitrary γ. If γ is an integer, however, we can use the binomial expansion and write down an expression for H_0 as a polynomial in the action $J = r^2/2$:

$$H_0(J) = \sum_{k=1}^{\gamma+1} c_k(\gamma) \left(\frac{J}{J_a}\right)^k, \tag{A.5}$$

in which $J_a = a^2/2$ and the coefficients are

$$c_k(\gamma) = \frac{J_a}{q_a} \frac{(-1)^{k+1}}{k} \frac{(\gamma+1)!}{k!(\gamma+1-k)!}. \tag{A.6}$$

Now, for the perturbation, consider the effect of a RHW with m equally spaced pairs of windings, that close on themselves after n turns along the poloidal direction, conducting a current I_H in opposite directions for adjacent conductors. Suppose that that the magnetic field $\mathbf{b}^{(1)}$ so created is a vacuum field (we neglect the plasma response and assume that the penetration time of the metallic wall is short enough), hence $\mathbf{b}^{(1)} = \nabla\Phi$, where Φ is a magnetic scalar potential satisfying Laplace's equation

$$\nabla^2\Phi(r,\theta,\phi) = 0. \tag{A.7}$$

Its solution, for $r < b$, is well-known and given by [31]

$$\Phi(r,\theta,\phi) = \frac{2\mu_0 I_H nb}{\pi R_0} \sum_{Nm=1}^{\infty} K'_{mN}\left(\frac{Nnb}{R_0}\right) I_{mN}\left(\frac{Nnr}{R_0}\right) \sin[N(m\theta - n\phi)] \tag{A.8}$$

where $N = 2p+1$, for $p = 0, 1, 2\ldots$, $K_\mu(x)$ and $I_\mu(x)$ are modified Bessel functions of order μ. Assuming $r \ll R_0$ and $b \ll R_0$ we can use the asymptotic expressions:

$$I_\mu(x) \overset{x\ll 1}{\sim} \frac{1}{\Gamma(\mu+1)}\left(\frac{x}{2}\right)^\mu, \tag{A.9}$$

$$K_\mu(x) \overset{x\ll 1}{\sim} \frac{\Gamma(\mu)}{2}\left(\frac{2}{x}\right)^\mu, \tag{A.10}$$

from which there results

$$\Phi(r,\theta,\phi) \approx -\frac{\mu_0 I_H}{\pi} \sum_{p=0}^{\infty} \frac{1}{2p+1}\left(\frac{r}{b}\right)^{m(2p+1)} \sin[(2p+1)(m\theta - n\phi)]. \tag{A.11}$$

For $r < b$, the magnitude of the terms in this summation decrease very fast with p, so that it suffices to retain only the lowest order term

$$\Phi(r,\theta,\phi) \approx -\frac{\mu_0 I_H}{\pi}\left(\frac{r}{b}\right)^m \sin(m\theta - n\phi), \tag{A.12}$$

in such a way that the Fourier coefficient of the radial component of the perturbing field, $b_r^{(1)}$, is given by

$$b_{rmn}(r) = i\frac{\mu_0 I_H}{\pi b}\left(\frac{r}{b}\right)^{m-1}. \tag{A.13}$$

References

[1] J. P. Friedberg. Ideal Magnetohydrodynamics, Plenum Press, New York, 1987.

[2] J. Wesson. Tokamaks. Oxford University Press, Oxford, 1987.

[3] A. Vannucci, I.C. Nascimento, I.L. Caldas, Disruptive instabilities in the discharge of the TBR-1 Tokamak, Plasma Physics and Controlled Fusion 31 (1989) 147–156.

[4] F. Karger, H. Wobig, S. Corti, J. Gernhardt, O. Klüber, G. Lisitano, K. McCormick, D. Meisel, S. Sesnick, Sixth International Conference on Plasma Physics and Controlled Nuclear Fusion Research, IAEA, Vienna, vol. 1, 1975, 207.

[5] I.L. Caldas, J.M. Pereira, K. Ullmann, R.L. Viana, Magnetic field line mappings for a Tokamak with ergodic limiters, Chaos, Solitons and Fractals 7 (7) (1996) 991–1010.

[6] W. Feneberg, The use of external helical windings for the production of a screening layer in ASDEX and a TOKAMAK with a material limiter, Proceedings of the Eighth European Conference of Contr. Fus. and Plas. Phys. 1 (1977) 3.
[7] I.H. Tan, I.L. Caldas, I.C. Nascimento, R.P. Silva, E.K. Sanada, R. Bruha, Mirnov oscillations in a small Tokamak, IEEE Transactions on Plasma Science PS-14 (3) (1986) 279–281.
[8] K.M. McGuire, D.C. Robinson, Magnetic islands and disruptions in a Tokamak, Proceedings of the European Conference on Controlled Fusion and Plasma Physics 1 (1979) 93.
[9] D.C. Robinson, Ten years of results from the TOSCA device, Nuclear Fusion 25 (1985) 1101–1108.
[10] J.M. Finn, The destruction of magnetic surfaces in Tokamaks by current perturbations, Nuclear Fusion 15 (1975) 845.
[11] M.V.A.P. Heller, I.L. Caldas, A. S. The destruction of magnetic surfaces by resonant helical windings, Plasma Physics and Controlled Fusion 30 (10) (1988) 1203–1211.
[12] L.H.A. Monteiro, V. Okano, M.Y. Kucinski, I.L. Caldas, Magnetic structure of toroidal helical fields in Tokamaks, Physics Letters A 193 (1994) 89–93.
[13] D.W. Kerst, The influence of errors on plasma-confining magnetic fields, Journal of Nuclear Energy 4C (1962) 253.
[14] N.N. Filonenko, R.Z. Sagdeev, G.M. Zaslawsky, Destruction of magnetic surfaces in Tokamaks by magnetic field irregularities: Part II, Nuclear Fusion 7 (1967) 253–256.
[15] R.P. Freis, C.W. Hartman, F.M. Hamzeh, A.J. Lichtenberg, Magnetic island formation and destruction in a Levitron, Nuclear Fusion 13 (1973) 533–548.
[16] F.M. Hamzeh, Magnetic surface destruction in toroidal systems, Nuclear Fusion 14 (1974) 523–536.
[17] K.J. Whiteman, Invariants and stability in classical mechanics, Reports on Progress in Physics 40 (1977) 1033–1069.
[18] R.L. Viana, Comment on a Hamiltonian representation for helically symmetric magnetic fields, Plasma Physics and Controlled Fusion 36 (1994) 587–588.
[19] R.L. Viana, Hamiltonian representation for magnetic field lines in an exactly soluble model, Brazilian Journal of Physics 25 (3) (1995) 215–218.
[20] R.L. Viana, D.B. Vasconcelos, Field-line stochasticity in a Tokamak with an ergodic magnetic limiter, Dynamics and Stability of Systems 12 (2) (1997) 75–88.
[21] A.J. Lichtenberg, M.A. Lieberman, Regular and Stochastic Motion, Springer, NY–Berlin–Heidelberg, 1983.
[22] A.J. Lichtenberg, Stochasticity as the mechanism for the disruptive phase of the $m = 1$ Tokamak oscillations, Nuclear Fusion 24 (10) (1984) 1277–1289.
[23] A.J. Lichtenberg, K. Itoh, S.-I. Itoh, A. Fukuyama, The role of stochasticity in sawtooth oscillations, Nuclear Fusion 32 (3) (1992) 495–512.
[24] H. Goldstein, Classical Mechanics, Addison Wesley, NY, 1980.
[25] B.V. Chirikov, A universal instability of many-dimensional oscillator systems, Physics Reports 52 (1979) 265–379.
[26] D.F. Escande, Stochasticity in classical Hamiltonian systems: universal aspects, Physics Reports 121 (3–4) (1985) 165–261.
[27] J.M. Greene, A method for determining a stochastic transition, Journal of Mathematical Physics 20 (1979) 1183–1201.
[28] I.C. Nascimento, I.L. Caldas, R.M.O. Galvão, Tokamak research at University of Sao Paulo, Journal of Fusion Energy 12 (1994) 529.
[29] D.F. Escande, M.S. Mohamed-Benkadda, F. Doveil, Threshold of global stochasticity and universality in Hamiltonian systems, Physics Letters 101A (7) (1984) 309–313.
[30] M.Y. Kucinski, I.L. Caldas, Toroidal helical fields, Zeitschrift fũr Naturforschung 42a (1987) 1124–1132.
[31] M.I. Morozov, L.S. Solovev, The structure of magnetic fields, in Reviews of Plasma Physics (Ed. M.A. Leontovich), 2, Consultants Bureau, NY, 1966.